Carbohydrate Polymers 92 (2013) 1249–1255

Contents lists available at SciVerse ScienceDirect

Carbohydrate Polymers

journal homepage: www.elsevier.com/locate/carbpol

# Structural variation of rice starch in response to temperature during microwave heating before gelatinisation

Daming Fan[b], Liyun Wang[b], Shenyan Ma[b], Wenrui Ma[b], Xiaoming Liu[b], Jianlian Huang[c], Jianxin Zhao[b], Hao Zhang[b], Wei Chen[a,b,*]

[a] State Key Laboratory of Food Science and Technology, Jiangnan University, Wuxi 214122, China
[b] School of Food Science and Technology, Jiangnan University, Wuxi 214122, China
[c] Fujian Anjoyfood Share Co. Ltd., Xiamen 361000, China

ARTICLE INFO

*Article history:*
Received 6 June 2012
Received in revised form 18 October 2012
Accepted 22 October 2012
Available online 29 October 2012

*Keywords:*
Rice starch
Subgelatinisation
Heating rate
Thermogravimetry
Differential scanning calorimetry
Small-angle X-ray scattering

ABSTRACT

Although it is well known that structural variations occur in starch during gelatinisation, little is known about how the structure of starch changes at subgelatinisation levels. The objective of this study was to investigate structural variations of rice starch ascribed to the temperature during microwave heating. Rapid conduction heating was used to imitate the high microwave heating rate through oil bath, which was then compared with traditional conduction heating. Structural changes due to temperature increases were investigated using thermogravimetry and differential scanning calorimetry while the distinct lamellar organisation of starch was obtained through small-angle X-ray scattering. The results showed that the structure of starch responds non-monotonically to temperature rising before gelatinisation, which was also affected by heating rates. The samples treated by microwave and rapid conduction heating essentially underwent the same thermal property changes and the molecular vibration of the microwaves did influence the submicroscopic lamellar structure.



## 1. Introduction

Starch constitutes a major component of many foods. Changes in the structures of starch granules can lead to variations in physical properties on a macroscopic scale (e.g., rheology), which influence the quality and processing of starch-based food products (Aggarwal & Dollimore, 1998; Blazek & Gilbert, 2011; Colonna, Tayeb, & Mercier, 1989). Hence, studies that focus on the structural changes in starch granules during food processing are of great significance in improving and controlling the quality of food.

The structure of a native starch granule is defined in terms of amorphous and semi-crystalline growth rings (Vandeputte, Vermeylen, Geeroms, & Delcour, 2003). Linear amylose molecules and probably less ordered amylopectin are present in an amorphous state within each native granule (Morrison, 1995; Primo-Martin, Van Nieuwenhuijzen, Hamer, & Van Vliet, 2007). Every semi-crystalline growth ring is composed of repeats of alternating amorphous and crystalline lamellae (Barsby, Donald, & Frazier, 2001), which are related to branch points of the amylopectin side chains and the short-chain fractions of amylopectin arranged as double helices and packed in small crystallites, respectively (Imberty, Buléon, Tran, & Péerez, 1991; Svensson & Eliasson, 1995; Tester, Karkalas, & Qi, 2004; Vandeputte et al., 2003). The semi-crystalline nature of starch is ascribed to the double helices formed by the hydrogen bond interactions of the amylopectin branches (Blazek & Gilbert, 2011; Fitzgerald, 2004; Hizukuri, 1986). Therefore, the strength of its hydrogen bonds largely determines the structure of a starch granule.

During the traditional processing of starch-based materials, starch granules are often treated using physical fields such as conduction heating or electromagnetic radiation. Hence, the interactions among hydrogen bonds within starch molecules are often affected through changes of orientation or intensity, resulting in changes in the semi-crystalline structure of starch. Studies have recently examined changes in the structure of starch granules in response to the relevant physical fields. Liu et al. (2009) reported that high-pressure processing at up to 10.0 MPa was not sufficient to destroy the crystalline structure of waxy corn starch molecules during gelatinisation process. Palav and Seetharaman (2007) found that the granules ruptured and there was a lack of swelling in starch at gelatinisation levels, when wheat starch dispersions were treated using microwave heating. However, little literature includes the studies investigating the response of hydrogen bond interactions to heating at subgelatinisation temperatures.

*Abbreviations:* MV, microwave heating; RCV, rapid conventional heating; CV, conventional heating.

* Corresponding author. Tel.: +86 0510 85912155; fax: +86 0510 85912155.
*E-mail address:* weichen@jiangnan.edu.cn (W. Chen).

0144-8617/$ – see front matter © 2012 Elsevier Ltd. All rights reserved.
http://dx.doi.org/10.1016/j.carbpol.2012.10.053

We focus on the effect of microwave heating on the starch during subgelatinisation, which is defined as the process in which the final temperature is lower than the temperature at which gelatinisation begins ($T_o$) for raw rice starch measured by DSC. However, the effect of microwave heating on starch granules has typically either been related to the fast heating rate, as reported by Bilbao-Sáinz, Butler, Weaver, and Bent (2007), or to the strong vibrational motion of the polar molecules (Palav & Seetharaman, 2006). Therefore, in this study, an oil bath (RCV) was used to imitate the high heating rate seen in microwave heating, to develop a better understanding of structural changes in rice starch granules at subgelatinisation temperatures when treated with microwave heating (MV), rapid conventional heating (RCV) and conventional conduction heating (CV).

## 2. Materials and methods

### 2.1. Materials

Rice starch (protein content ≤ 0.23%, starch content ≥ 94.22%, amylose content of 15.11%, particle size of 5.52 ± 0.23 μm) was isolated and purified from fresh rice (QiuShouBao Rice Products Co., Ltd., Anhui, China), as described in the previous works (Fan, Ma, Wang, Huang, et al., 2012; Fan, Ma, Wang, Zhao, et al., 2012).

### 2.2. Methods

#### 2.2.1. Heating conditions

*2.2.1.1. Rapid conventional heating (RCV).* A thermostat (Thermo Fisher Scientific Co., Ltd., MA, USA) with an oil bath (200 °C) was used for rapid heating. The starch suspensions (100 g) with a concentration of 6% (w/w) were prepared with distilled water and heated to the desired temperature in the oil bath under constant agitation using an agitator (RW20, IKA Co., Ltd., Germany). The temperature was monitored online using an optical fibre probe (FISO Technologies Inc., Québec, Canada). The suspensions were then immediately placed into an ice bath to stop the gelatinisation process. The treated suspensions were freeze-dried, and then the starch samples were smashed in order to pass through a 75-μm sieve.

*2.2.1.2. Microwave heating (MV).* The MV experiment was conducted in the same manner as that described above, except a microwave oven was used for heating. A 2450 MHz oven (Xianou Instrument Manufacturing Co., Ltd., Nanjing, China) was used to match the heating rate obtained in the conventional heating using an oil bath. Multiple replications were performed in the preliminary stages to determine the power necessary to match the oil bath.

*2.2.1.3. Conventional heating (CV).* The CV experiment was conducted in the same manner as that described above, except that the sample mass was increased to 200 g and a hot plate was used for heating. Its measured heating rate was 0.13 °C/s.

#### 2.2.2. Thermal analyses

*2.2.2.1. Thermogravimetry.* The thermogravimetric analysis was performed with a Mettler-Toledo TGA/SDTA851E (Mettler-Toledo AG, Greifensee, Switzerland). The operation was conducted from 30 to 700 °C at heating rates of 5, 10, 15 and 20 °C/min under nitrogen, and a sample mass of 5 mg was maintained throughout the test. The thermogravimetric data were analysed according to BS ISO 11358-2 (British Standard Institution, 2005).

*2.2.2.2. Differential scanning calorimetry.* The starch sample heated to different final temperatures was analysed with a Q2000 differential scanning calorimeter (TA Instruments, New Castle, USA).

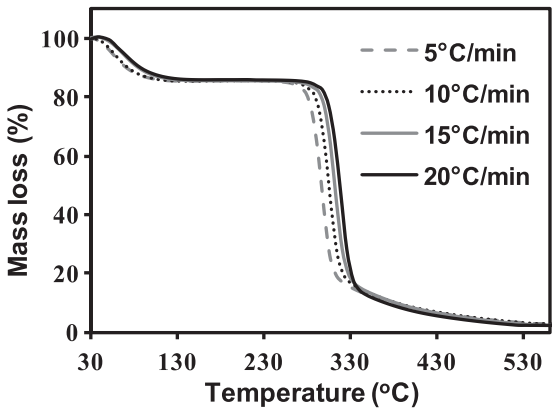


**Fig. 1.** Thermogravimetry curves of MV40 °C (starch heated by microwave to 40 °C) at heating rates of 5, 10, 15 and 20 °C/min.

Approximately 8–10 mg of the freeze-dried sample was weighed into a standard aluminium sample pan. Each sample was scanned from 30 to 90 °C at the rate of 10 °C/min. A sealed empty pan was used as a reference.

*2.2.3. Small-angle X-ray scattering*

SAXS experiments were performed on a SAXSess mc$^2$ nanostructure analyser (Anton Paar, Austria) with an incident X-ray monochromatic beam ($\lambda_{CuK\alpha}$ = 1.54 Å) monitored by a photomultiplier. The rotating anode device was operated at 40 kV and 50 mA. Scattering was detected in the range defined by the scattering vector $q$ [$q = 4\sin(\theta)/\lambda$, with $\lambda$ being the wavelength and $\theta$ the scattering angle] 0.04–2.70 nm$^{-1}$. Transmission, dark current and aluminium foil corrections were performed on the 2D images before further data processing. The data were analysed after desmearing with SAXSQuant software (Anton Paar, Austria). Dried starch samples were weighed (8.0 ± 0.3 mg) and placed on the aluminium foils. Water was carefully added (8 μL) to the starch and the samples were sealed to prevent any change in the amount of water present during the experiments (Cardoso & Westfahl, 2010). Measurements were performed at room temperature and each SAXS pattern was cumulated for 7 min.

All analyses were conducted in triplicate and the average values were reported.

## 3. Results and discussion

### 3.1. Comparison of heating rates between MV and RCV

Our previous study focusing on the gelatinisation of rice starch heated by MV compared the time–temperature profiles for MV and RCV below 85 °C (Fan, Ma, Wang, Huang, et al., 2012; Fan, Ma, Wang, Zhao, et al., 2012). In those results, above 70 °C, the heating rate of RCV decreased, while that of MV increased. Hence, we had to use the multi-stage MV heating program to match the profile of RCV. However, the highest heating temperature in this study was 70 °C, therefore only one microwave power (1.2 kW) was used here. The time–temperature curves for MV and RCV completely coincided, and the heating rate of both MV and RCV was 1.12 °C/s (the figure of temperature curves was not shown).

### 3.2. Thermal property analysis

#### 3.2.1. Thermogravimetry (TG)

The activation energy (Ea) analysed from TG thermograms (Fig. 1) was used to describe the thermal stability caused by different heating methods (Guinesi et al., 2006; Marques et al., 2006). The

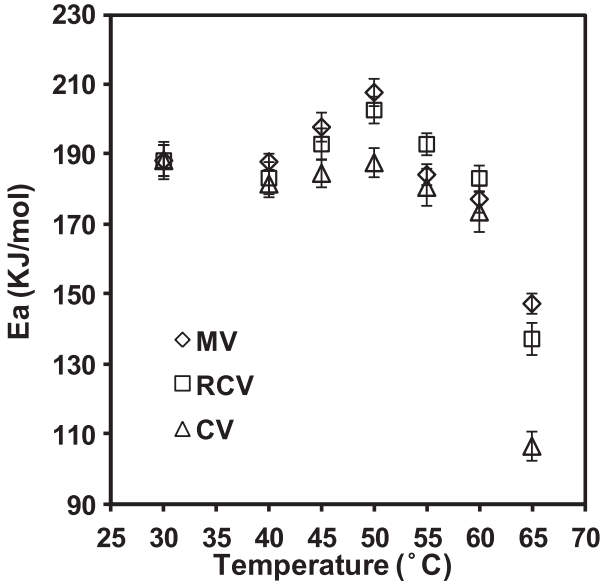


**Fig. 2.** Activation energy (Ea) values versus sample temperatures after rapid conventional (RCV), microwave (MV) and conventional (CV) heating.

results of Ea determined through Arrhenius plot (British Standard Institution, 2005) with a 60% mass loss, were shown in Fig. 2. It was observed that the activation energy initially increased before decreasing as the heating temperature rose below the subgelatinisation temperature. The Ea changes were more significant in the starch suspensions treated by RCV and MV, for which the values were always higher than those of the samples heated by CV at every temperature measured, suggesting a higher degree of thermal stability in starch heated at a rapid rate. Moreover, the similarity of activation energy results between samples treated by MV and RCV indicated that most of the effect of microwaves on the starch before gelatinisation might be reflected in the change in the rapid heating rate. The structural changes were also identified in terms of Ea values, among which the differences might be associated with intermolecular interactions and the strength of chemical bonds reflected through infrared spectroscopy (IR) (Marques et al., 2006; Sin, Rahman, Rahmat, & Mokhtar, 2011; Wang et al., 2012). Clearly, the peak Ea value of 50 °C for the samples subjected to RCV and MV show the reinforcement of hydrogen bonds and a higher level of chemical bond energy in groups within the starch granules at the beginning of the rapid heating process. This behaviour is consistent with previous results showing that the chemical groups of starch molecules heated by MV and RCV, such as C—O, C—H and skeletal types (C—C and glycosidic linkages, etc.) obtained by IR spectra, all experienced maximum absorption intensity at 50 °C (Fan, Ma, Wang, Huang, et al., 2012). Hence, it could be concluded that rapid heating had an enhanced effect on the stability of starch molecules in the initial heating stage.

### 3.2.2. *Differential scanning calorimetry*

The endothermic enthalpy ascribed to the loss of ordered structure, i.e. the double helices, in amylopectin (Kohyama & Sasaki, 2006) was quantified by the DSC measurements (Fig. 3). The enthalpy values ($\Delta H$) of the samples treated by RCV were almost identical to those of samples heated by MV at every temperature point measured (Fig. 4). The enthalpy values initially increased to a maximum at 50 °C before decreasing as the temperature rose further, as described above in relation to the activation energy issue. The similarity of the results from the samples heated by RCV and MV suggested that a rapid heating rate might be the most influential factor in microwave heating, which was consistent with previously

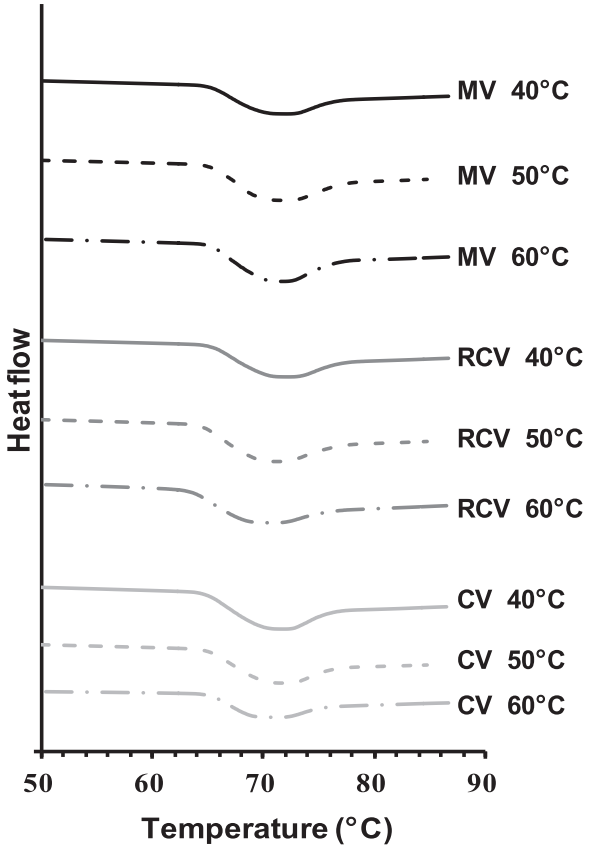


**Fig. 3.** Differential scanning calorimetry (DSC) profiles of rice starch samples treated by rapid conventional (RCV), microwave (MV) and conventional (CV) heating.

reported results (Bilbao-Sáinz et al., 2007). The critical peaks for both TG and DSC at 50 °C indicated that crystalline structures had diverse responses to a rising temperature, and showed that a rapid heating rate could enhance the strength of hydrogen bond interactions in amylopectin in the early stages of processing (Kohyama & Sasaki, 2006).

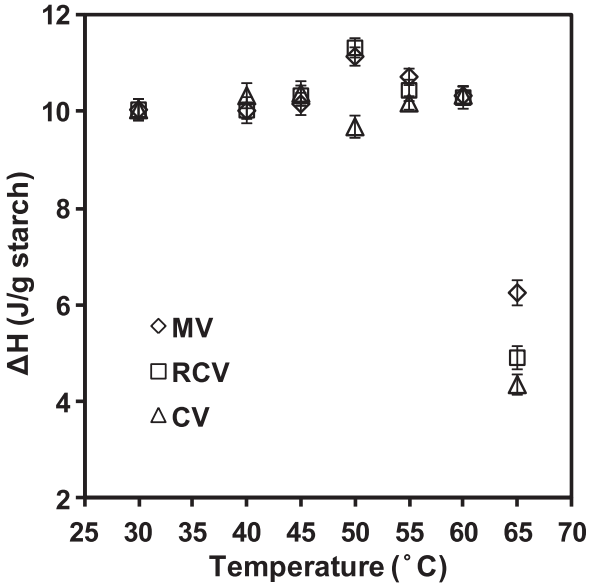


**Fig. 4.** Gelatinisation enthalpy values ($\Delta H$) versus sample temperatures after rapid conventional (RCV), microwave (MV) and conventional (CV) heating.

The measurements of the three samples at 50 °C were distinct. The enthalpy curves (Fig. 4) of the sample subjected to MV and RCV showed positive peaks (i.e., increased first and decreased afterwards), whereas those treated by CV showed a reverse change around 50 °C, which indicated that the heating rate may have an effect on the changes in the crystal structure before gelatinisation. Compared with the samples conducted by MV and RCV, those treated by CV took longer to reach the final temperature, which might lead to a decrease in the strength of the hydrogen bonds and the value of enthalpy in the initial heating stage. The behaviour of enthalpy curve related to CV required further exploration.

### 3.3. SAXS analysis

Advances in the quantification of the lamellar repeats architecture of the semi-crystalline growth rings formed by alternating crystalline and amorphous regions in the structure of starch granules can be obtained using the SAXS technique (Cardoso & Westfahl, 2010). Due to the semi-crystalline nature of starch granules, which was ascribed to the amylopectin, DSC and SAXS have been used in parallel to reveal the complex ultrastructure of such granules (Blazek & Gilbert, 2011). Therefore, SAXS experiments were conducted to explore possible reasons for the special peaks in the structure scale.

#### 3.3.1. SAXS curves

The SAXS patterns of all of the samples were expressed as intensity as a function of the scattering vector modulus $q$ (Fig. 5). Fig. 5a–c reported similar results, all of which showed a marked decrease in peak intensity when the final temperature was above 50 °C. This fall in scattering intensity as the temperature rose was in agreement with the observations made by Silveira et al. (Cardoso, Samios, & Silveira, 2006; Thys et al., 2008), who focused on the subgelatinisation of starch throughout alkaline treatment. They also found that the peak intensity dropped as the starch extraction proceeded using alkaline or as the treating NaOH concentration was increased. Hence, it was concluded that the amorphisation of the crystalline lamellae would lead to a decrease in peak intensity. The effects of heat on starch granules under temperatures above 50 °C might also be attributed to the dissociation of hydrogen bonds inside the starch granule (Cardoso et al., 2006; Thys et al., 2008). However, such heating could cause total gelatinisation (above 70 °C) rather than partial amorphisation through alkaline processing. According to Cameron and Donald (1993), the heating could reduce the contrast between the crystalline and amorphous lamellae. Therefore, the absolute intensity of the peak decreased.

#### 3.3.2. Lamellar repeat distance (D)

There was a broad scattering peak in the range of $q$ 0.60–0.70 $nm^{-1}$, reciprocally revealing the position related to the average total thickness of the crystalline and amorphous regions in the lamellar arrangement in rice starches, i.e. the lamellar repeat distance, long period or Bragg spacing. The $q$ value of the peak (below 65 °C) remained almost unchanged, tentatively indicating that the lamellar repeat distance of starch does not change according to the heating method or the final temperature (see Fig. 4). Other researchers have also found that the heating does not cause a shift in the position of the peak during gelatinisation (Jenkins et al., 1994; Jenkins & Donald, 1997; Perry & Donald, 2002; Waigh, Gidley, Komanshek, & Donald, 2000). The following quantitative analysis was undertaken to analyse the lamellar repeat distance in detail. Scattering was characterised by the law of reciprocity, which presented an inverse relationship between the size or dimension of the scattering object and its associated scattering angle (Blazek & Gilbert, 2011). The lamellar repeat distance (one crystalline + one amorphous lamella) $D$ was calculated via Bragg's law to yield a real-space dimension with spacing at the scattering peak intensity $D = 2\pi/q_p$ (Engel, Stühn, Schneider, Cornelius, & Naumann, 2009; Putseys, Gommes, Puyvelde, Delcour, & Goderis, 2011) and $q_p$ being the modulus of the scattering vector at peak intensity. Before being heated to 65 °C, all of the starch samples had an almost identical main SAXS peak at an approximate scattering maximum of 9–10 nm, consistent with earlier reports on rice starch (Cardoso et al., 2006; Koroteeva et al., 2007; Vandeputte and Delcour, 2004). A subtle distinction was only observed when the maximum peak positions were compared (Table 1). The data show that the different heating methods did not lead to obvious variations in the average thickness of the amylopectin cluster (Cardoso & Westfahl, 2010)

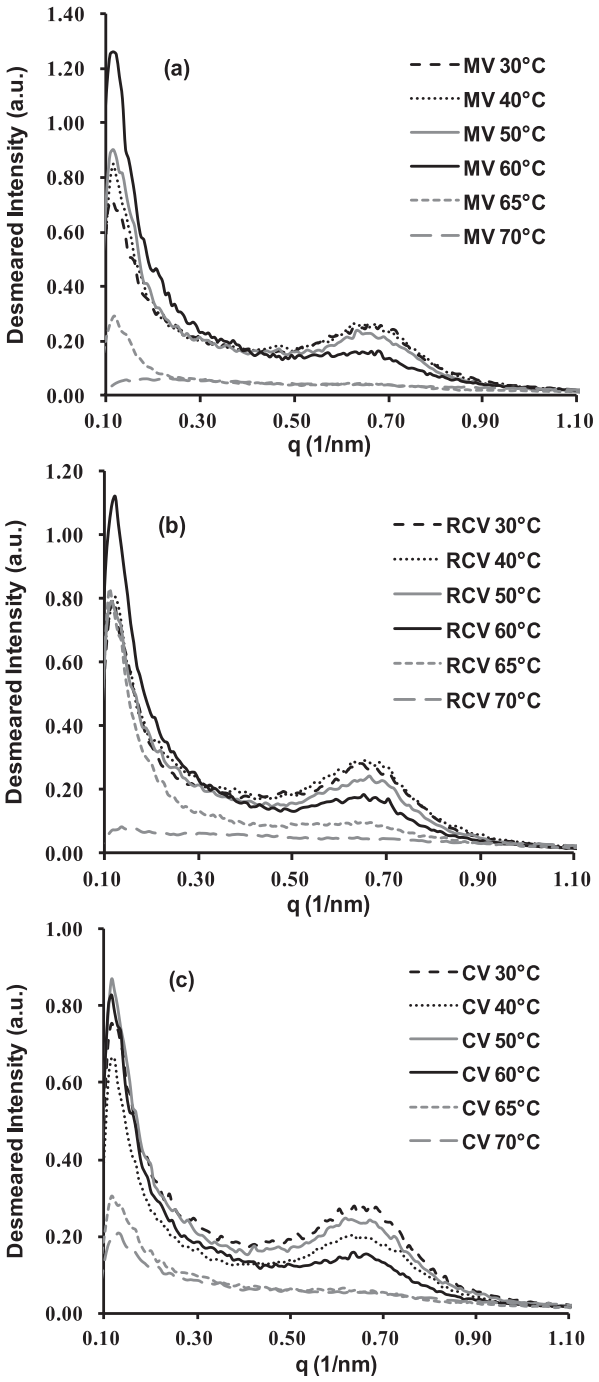


**Fig. 5.** Small-angle X-ray scattering (SAXS) patterns of starch samples conducted by rapid conventional (RCV), microwave (MV) and conventional (CV) heating.

**Table 1**
The lamellar repeat distance and thickness of transition layer of samples conducted by rapid conventional (RCV), microwave (MV), and conventional (CV) heating.

| Sample temperature (°C) | $D$ (nm)[a] | | | $\sigma$ (nm)[b] | | |
|---|---|---|---|---|---|---|
| | MV | RCV | CV | MV | RCV | CV |
| Native starch | | 9.54 ± 0.03 | | | 1.30 ± 0.02 | |
| 30 | 9.54 ± 0.02 | 9.60 ± 0.03 | 9.58 ± 0.03 | 1.29 ± 0.06 | 1.29 ± 0.01 | 1.29 ± 0.04 |
| 40 | 10.04 ± 0.04 | 9.67 ± 0.03 | 9.93 ± 0.03 | 1.39 ± 0.00 | 1.23 ± 0.02 | 1.30 ± 0.08 |
| 45 | 9.98 ± 0.05 | 9.57 ± 0.04 | 10.04 ± 0.13 | 1.37 ± 0.01 | 1.22 ± 0.02 | 1.27 ± 0.03 |
| 50 | 9.93 ± 0.06 | 9.48 ± 0.09 | 10.14 ± 0.08 | 1.35 ± 0.00 | 1.20 ± 0.07 | 1.24 ± 0.04 |
| 55 | 9.60 ± 0.02 | 9.62 ± 0.00 | 9.99 ± 0.03 | 1.04 ± 0.02 | 1.06 ± 0.02 | 1.12 ± 0.01 |
| 60 | 9.26 ± 0.11 | 9.76 ± 0.02 | 9.83 ± 0.07 | 0.74 ± 0.05 | 0.91 ± 0.03 | 1.00 ± 0.00 |
| 65 | ND[c] | ND | ND | CNC[d] | CNC | CNC |
| 70 | ND | ND | ND | CNC | CNC | CNC |

[a] Bragg lamellar repeat distance.
[b] The thickness of transition layer.
[c] No scattering maximum detectable in the desmeared SAXS pattern.
[d] Cannot be calculated.

during the subgelatinisation process. The invariance of the lamellar repeat distance as the temperature increased also confirmed the view that the semicrystalline growth ring did not expand radially during heating (Jenkins et al., 1994; Jenkins & Donald, 1997).

### 3.3.3. Approximate invariant ($Q_{ap}$) and thickness of transition layer ($\sigma$)

After the subtraction of a constant liquid-scattering term, the mean square fluctuation of electron density in the stacked lamellae was approximated by integrating the smeared intensities $\tilde{I}(q)$ in the range of $q$ 0.07–0.70 nm$^{-1}$: $Q_{ap} = \int \tilde{I}(q) q\, dq$, where $Q_{ap}$ was the 'approximate' invariant (Vermeylen, Goderis, Reynaers, & Delcour, 2004). This resulted mainly from the difference between the crystalline and amorphous phases in the semi-crystalline growth rings (Vermeylen, Goderis, & Delcour, 2006). However, it is noteworthy that in Flory's theory, a 'third phase' (i.e. interphase) exists between the crystalline and amorphous regions in crystal polymers (Flory, Yoon, & Dill, 1984). Moreover, the samples analysed by Porod's law (Zhu, 2008) were found to have a negative deviation in the $\ln[q^4\tilde{I}(q)]$ versus $q^2$ curve when $q$ was greater than a certain value, suggesting the presence of a transition layer in the starch semicrystalline structure (Zhao et al., 2002). Hence, the total scattering power, or invariant $Q_{ap}$, of the three phase systems was described by correction Eq. (1) (Goderis, Reynaers, Koch, & Mathot, 1999; Zhu, 2008):

$$Q_{ap} \propto (\rho_A - \rho_B)^2 \left(\varphi_A\varphi_B - \frac{\varphi_C}{6}\right) \quad (1)$$

Here, the electron density of the crystalline and amorphous lamellae was denoted by $\rho_A$ and $\rho_B$, respectively, with $(\rho_A - \rho_B)$ representing the electron density difference between the crystalline and amorphous lamellae in the stack with $\varphi_A$, $\varphi_B$ and $\varphi_C$ being the volume fraction of the crystalline, amorphous lamellae and interphase in the lamellar stack, respectively, and $\varphi_A + \varphi_B + \varphi_C = 1$.

Although it could be concluded that $Q_{ap}$ had a positive correlation with the electron density difference, it also had a complicated relationship with the changes in the transition layer. Thus, the thickness of the transition layer ($\sigma$) was computed by following Porod' s law (Zhu, 2008), which reflects the $\varphi_C$ value.

The $Q_{ap}$ and $\sigma$ values of the starch samples heated to different final temperatures are presented in Table 1 and Fig. 6. The differences between the crystalline and amorphous phases followed a generally decreasing trend as the heating temperature rose. In addition, the thickness of the transition layer could not be calculated after a sample was heated to 60 °C, indicating that the transition layer had disappeared and that there was no significant difference in the phase system due to the cluttered side chain of amylopectin. Therefore, the changes in the lamellar repeat architecture of amylopectin, reflected by $Q_{ap}$ and $\sigma$, were consistent with the current understanding of the gelatinisation process (Jenkins & Donald, 1998; Palav & Seetharaman, 2006; Sakonidou, Karapantsios, & Raphaelides, 2003).

The samples treated by MV and RCV followed a similar pattern of $Q_{ap}$ changes. However, there was an obvious difference in $\sigma$ values, suggesting that although starch could acquire similar thermal properties in a macroscopic view when heated at the same rate, its lamellar repeats structure of semi-crystalline growth rings was still affected by the molecular vibration of microwave heating. It was noted that at the beginning of MV, the values of $\varphi_C$ and $Q_{ap}$ both increased as the temperature rose, reaching a maximum at 40 °C. Because the sum of $\varphi_A$, $\varphi_B$ and $\varphi_C$ was constant, the increase in $\varphi_C$ implied either a decrease in $\varphi_A$ and $\varphi_B$ or a fall in the sum of $\varphi_A$ and $\varphi_B$. Hence, the value of $(\varphi_A\varphi_B - \varphi_C/6)$ decreased. It could be concluded that the increase in $Q_{ap}$ was due to the increase in the electron density difference between the amorphous and crystalline lamellae in the stack during the initial microwave heating process, as expressed by Eq. (1). Despite the similarity in $Q_{ap}$ values at 40 °C, the thickness of the transition layer ($\varphi_C$) decreased during RCV processing, which might not produce the same conclusion about the difference between the two phases. It was previously thought that the interphase contributed only marginally to the scattering pattern in the angular region (Crist, 2000; Vermeylen et al.,

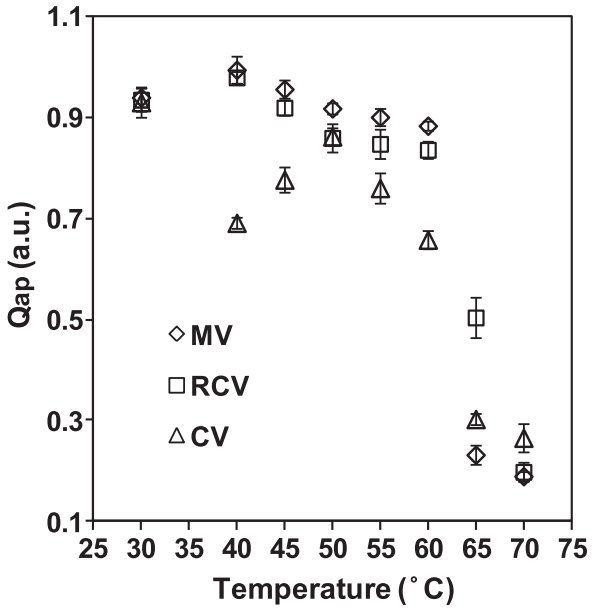


**Fig. 6.** 'Approximate' invariant values ($Q_{ap}$) versus sample temperatures after rapid conventional (RCV), microwave (MV) and conventional (CV) heating.

2004). Hence, it could be also accepted that its electron density contrast increased in the initial stage of RCV. The increase in $(\rho_A - \rho_B)$ might be due to a number of different reasons, such as an increase in $\rho_A$ or a decrease in $\rho_B$. A number of other studies (Jenkins et al., 1994; Jenkins & Donald, 1997, 1998; Perry & Donald, 2002) had reported the increase of $(\rho_A - \rho_B)$ in SAXS experiments on starch during gelatinisation. They concluded that the increase in the difference between crystalline and amorphous lamellae was due to a reduction in the value of $\rho_B$, because the peak point of $(\rho_A - \rho_B)$ occurred after the onset temperature of the DSC endotherm when the amorphous growth ring had reached water uptake saturation and more water was absorbed into the amorphous lamellae, resulting in a dramatic drop in $\rho_B$ (Cameron & Donald, 1993; Jenkins et al., 1994; Jenkins & Donald, 1997). However, the increased difference observed here might not be explained by the same reason. First, the MV and RCV heating rates were much faster than those in the above mentioned studies. Second, the changeover point of $(\rho_A - \rho_B)$ was at about 40 °C in this study, which was much lower than the onset temperature of the DSC endotherm (65.79 °C). Hence, insufficient time was available for the starch granules treated by MV and RCV to absorb adequate water and the electron density of the amorphous lamellae, $\rho_B$, remained unaffected (Perry & Donald, 2002). Therefore, in this study, the increased contrast between the crystalline and amorphous lamellae was due to the increase in $\rho_A$. Evidently, in the early stage of treatment, the rapid heating rate resulted in the double helices of amylopectin becoming more optimally or densely packed, which accounted for the more ordered crystalline lamellae (Tester & Debon, 2000). Vermeylen (Vermeylen et al., 2006; Vermeylen, Goderis, Reynaers, & Delcour, 2005) believed that this resulted from the fact that side chains of amylopectin behaved as a liquid crystalline polymer, with the plasticisation of amylopectin branch points acting as flexible spacers that allowed the double helices to become more precisely aligned in the crystalline lamellae. However, the invariant differences between the heating methods, rates and different final temperatures might not be clearly shown simply by using the model in the same starch and water determination conditions in which the transition from the nematic (possessing orientation order but lacking position order) to smectic (aligned in layers) phases occurred in all of the samples (Blazek & Gilbert, 2011). Therefore, it can be assumed that the rapid heating rate did affect the orientation and position of the double helices in the crystalline lamellae. Furthermore, it enhanced the strength of the hydrogen bonds in the amylopectin molecules, which were maximised at 40 °C. It has previously been proposed that the orientation of the polar group, —OH, in starch molecules is less hampered by chain segments when the temperature raised to 40 °C, which accounts for an easier dipole rotation and a weaker Brownian motion effect (Schubert & Regier, 2008; Zhao, 2008). Thus, new hydrogen bond links might be formed or the existing ones might be strengthened. However, the Brownian motion observed at higher temperatures (above 40 °C) in this study was more violent, resulting in increased interference with the dipole orientation and the destruction of intermolecular hydrogen bonding. Although this was also confirmed by the DSC and TG results, the analysis of thermal properties showed that the peak temperature was 50 °C, indicating that the macroscopic changes might be asynchronous to the submicroscopic lamellae structural changes.

A clear distinction was observed in the $Q_{ap}$ values of starch treated by the three heating methods at 40 °C. The samples heated by CV experienced a significantly negative peak, unlike the positive peaks observed in the samples treated by rapid heating methods. This finding was similar to the results of SAXS experiments on starch gelatinisation reported in a previous study (Cameron & Donald, 1993). This behaviour might be due to the individual effects of the fall in $\rho_A$ as the crystalline order was lost and the fall in $\rho_B$ as water was absorbed into the amorphous lamellae on $(\rho_A - \rho_B)$. Hence, the rate at which crystalline order was lost was higher than that at which water was absorbed into the amorphous lamellae in the initial stage of CV. The trend observed in the integrated scattering intensity as the temperature increased was completely consistent with that of DSC. The increasing level of thermal stability could also be explained by a denser packing of double helices; that is, a higher $Q_{ap}$ value (Cooke & Gidley, 1992; De Gennes & Pincus, 1977), as confirmed by the results and the inferences of DSC in light of the SAXS experiments.

## 4. Conclusions

The structure of starch responded non-monotonically to temperature rising before gelatinisation, that was, the influence of temperature on hydrogen bonding interactions in starch molecules differed during microwave heating: In the initial stage, the hydrogen bond strength within double helices was enhanced by temperature rising, while it was then destroyed by further heating. The critical point of macro-thermal properties was a temperature of 50 °C, which was higher than that of the lamellar architecture (40 °C).

The samples that were heated to every final temperature point by RCV and MV yielded similar results. It can be concluded that the effect of microwave heating on the macroscopic properties of starch granules was mainly attributable to the rapid heating rate rather than to the molecular vibration mechanism. The results of the CV experiments showed that the heating rate directly affects the strength of the hydrogen bonds in amylopectin with respect to their molecular and submicroscopic lamellar structure. Further studies are required to quantitatively analyse the effect of temperature on the lamellar repeats architecture. A better understanding of the specific changes that occur during heating will aid researchers in designing and improving the quality of starch-based food products.

## Acknowledgment

This research was supported by the National Science & Technology Pillar Program, No. 2008BAD91B03, from the Chinese Ministry of Education.

## References

Aggarwal, P., & Dollimore, D. (1998). A thermal analysis investigation of partially hydrolyzed starch. *Thermochimica Acta*, *319*, 17–25.
Barsby, T. L., Donald, A. M., & Frazier, P. (2001). *Starch: Advances in structure and function*. Cambridge: The Royal Society of Chemistry.
Bilbao-Sáinz, C., Butler, M., Weaver, T., & Bent, J. (2007). Wheat starch gelatinization under microwave irradiation and conduction heating. *Carbohydrate Polymers*, *69*(2), 224–232.
Blazek, J., & Gilbert, E. P. (2011). Application of small-angle X-ray and neutron scattering techniques to the characterisation of starch structure: A review. *Carbohydrate Polymers*, *85*, 281–293.
British Standard Institution. (2005). *Plastics – Thermogravimetry (TG) of polymers – Part 2: Determination of activation energy*. BS ISO 11358-2.
Cameron, R. E., & Donald, A. M. (1993). A small-angle X-ray scattering study of the absorption of water into the starch granule. *Carbohydrate Research*, *244*(2), 225–236.
Cardoso, M. B., Samios, D., & Silveira, N. P. (2006). Study of protein detection and ultrastructure of Brazilian rice starch during alkaline extraction. *Starch-Stärke*, *58*(7), 345–352.
Cardoso, M. B., & Westfahl, H., Jr. (2010). On the lamellar width distributions of starch. *Carbohydrate Polymers*, *81*(1), 21–28.
Colonna, P., Tayeb, J., & Mercier, C. (1989). Extrusion cooking of starch and starchy products. In *Extrusion cooking* (pp. 247–319).
Cooke, D., & Gidley, M. J. (1992). Loss of crystalline and molecular order during starch gelatinisation: Origin of the enthalpic transition. *Carbohydrate Research*, *227*, 103–112.
Crist, B. (2000). Analysis of small-angle X-ray scattering patterns. *Journal of Macromolecular Science, Part B*, *39*(4), 493–518.
De Gennes, P., & Pincus, P. (1977). Nematic polymers. *Polymer Preprints*, *18*, 161–166.
Engel, M., Stühn, B., Schneider, J. J., Cornelius, T., & Naumann, M. (2009). Small-angle X-ray scattering (SAXS) off parallel, cylindrical, well-defined nanopores: From

random pore distribution to highly ordered samples. *Applied Physics A: Materials Science & Processing*, *97*(1), 99–108.
Fan, D., Ma, W., Wang, L., Huang, J., Zhao, J., Zhang, H., et al. (2012). Determination of structural changes in microwaved rice starch using Fourier transform infrared and Raman spectroscopy. *Starch-Stärke*, *64*(8), 598–606.
Fan, D., Ma, S., Wang, L., Zhao, J., Zhang, H., & Chen, W. (2012). Effect of microwave heating on optical and thermal properties of rice starch. *Starch-Stärke*, *64*(9), 740–744.
Fitzgerald, M. (2004). Starch. In *Rice chemistry and technology* (pp. 109–141).
Flory, P. J., Yoon, D. Y., & Dill, K. A. (1984). The interphase in lamellar semicrystalline polymers. *Macromolecules*, *17*(4), 862–868.
Goderis, B., Reynaers, H., Koch, M., & Mathot, V. (1999). Use of SAXS and linear correlation functions for the determination of the crystallinity and morphology of semi-crystalline polymers. Application to linear polyethylene. *Journal of Polymer Science, Part B: Polymer Physics*, *37*(14), 1715–1738.
Guinesi, L. S., da Róz, A. L., Corradini, E., Mattoso, L. H. C., Teixeira, E. M., & Curvelo, A. A. S. (2006). Kinetics of thermal degradation applied to starches from different botanical origins by non-isothermal procedures. *Thermochimica Acta*, *447*(2), 190–196.
Hizukuri, S. (1986). Polymodal distribution of the chain lengths of amylopectins, and its significance. *Carbohydrate Research*, *147*, 342–347.
Imberty, A., Buléon, A., Tran, V., & Péerez, S. (1991). Recent advances in knowledge of starch structure. *Starch-Stärke*, *43*(10), 375–384.
Jenkins, P., Comerson, R., Donald, A., Bras, W., Derbyshire, G., Mant, G., et al. (1994). In situ simultaneous small and wide angle X-ray scattering: A new technique to study starch gelatinization. *Journal of Polymer Science, Part B: Polymer Physics*, *32*(8), 1579–1583.
Jenkins, P. J., & Donald, A. M. (1997). Breakdown of crystal structure in potato starch during gelatinization. *Journal of Applied Polymer Science*, *66*(2), 225–232.
Jenkins, P. J., & Donald, A. M. (1998). Gelatinisation of starch: A combined SAXS/WAXS/DSC and SANS study. *Carbohydrate Research*, *308*(1–2), 133–147.
Kohyama, K., & Sasaki, T. (2006). Differential scanning calorimetry and a model calculation of starches annealed at 20 and 50 °C. *Carbohydrate Polymers*, *63*(1), 82–88.
Koroteeva, D. A., Kiseleva, V. I., Krivandin, A. V., Shatalova, O. V., Błaszczak, W., Bertoft, E., et al. (2007). Structural and thermodynamic properties of rice starches with different genetic background. Part II: Defectiveness of different supramolecular structures in starch granules. *International Journal of Biological Macromolecules*, *41*, 534–547.
Liu, H., Yu, L., Dean, K., Simon, G., Petinakis, E., & Chen, L. (2009). Starch gelatinization under pressure studied by high pressure DSC. *Carbohydrate Polymers*, *75*(3), 395–400.
Marques, P., Lima, A., Bianco, G., Laurindo, J., Borsali, R., Le Meins, J. F., et al. (2006). Thermal properties and stability of cassava starch films cross-linked with tetraethylene glycol diacrylate. *Polymer degradation and stability*, *91*(4), 726–732.
Morrison, W. (1995). Starch lipids and how they relate to starch granule structure and functionality. *Cereal Foods World*, *40*(6), 437–446.
Palav, T., & Seetharaman, K. (2006). Mechanism of starch gelatinization and polymer leaching during microwave heating. *Carbohydrate Polymers*, *65*(3), 364–370.
Palav, T., & Seetharaman, K. (2007). Impact of microwave heating on the physicochemical properties of a starch–water model system. *Carbohydrate Polymers*, *67*(4), 596–604.
Perry, P., & Donald, A. (2002). The effect of sugars on the gelatinisation of starch. *Carbohydrate Polymers*, *49*(2), 155–165.
Primo-Martin, C., Van Nieuwenhuijzen, N., Hamer, R., & Van Vliet, T. (2007). Crystallinity changes in wheat starch during the bread-making process: Starch crystallinity in the bread crust. *Journal of Cereal Science*, *45*(2), 219–226.
Putseys, J., Gommes, C., Puyvelde, P. V., Delcour, J., & Goderis, B. (2011). In situ SAXS under shear unveils the gelation of aqueous starch suspensions and the impact of added amylose–lipid complexes. *Carbohydrate Polymers*, *84*, 1141–1150.
Sakonidou, E., Karapantsios, T., & Raphaelides, S. (2003). Mass transfer limitations during starch gelatinization. *Carbohydrate Polymers*, *53*(1), 53–61.
Schubert, H., & Regier, M. (2008). *The microwave processing of foods*. Beijing: China Light Industry Press.
Sin, L. T., Rahman, W. A. W. A., Rahmat, A. R., & Mokhtar, M. (2011). Determination of thermal stability and activation energy of polyvinyl alcohol–cassava starch blends. *Carbohydrate Polymers*, *83*, 303–305.
Svensson, E., & Eliasson, A. C. (1995). Crystalline changes in native wheat and potato starches at intermediate water levels during gelatinization. *Carbohydrate Polymers*, *26*(3), 171–176.
Tester, R. F., & Debon, S. J. J. (2000). Annealing of starch—A review. *International Journal of Biological Macromolecules*, *27*(1), 1–12.
Tester, R. F., Karkalas, J., & Qi, X. (2004). Starch—Composition, fine structure and architecture. *Journal of Cereal Science*, *39*(2), 151–165.
Thys, R. C. S., Westfahl, H., Jr., Norena, C. P. Z., Marczak, L. D. F., Silveira, N. P., & Cardoso, M. B. (2008). Effect of the alkaline treatment on the ultrastructure of C-type starch granules. *Biomacromolecules*, *9*(7), 1894–1901.
Vandeputte, G., & Delcour, J. (2004). From sucrose to starch granule to starch physical behaviour: A focus on rice starch. *Carbohydrate Polymers*, *58*(3), 245–266.
Vandeputte, G., Vermeylen, R., Geeroms, J., & Delcour, J. (2003). Rice starches. I. Structural aspects provide insight into crystallinity characteristics and gelatinisation behaviour of granular starch. *Journal of Cereal Science*, *38*(1), 43–52.
Vermeylen, R., Goderis, B., & Delcour, J. A. (2006). An X-ray study of hydrothermally treated potato starch. *Carbohydrate Polymers*, *64*(2), 364–375.
Vermeylen, R., Goderis, B., Reynaers, H., & Delcour, J. A. (2004). Amylopectin molecular structure reflected in macromolecular organization of granular starch. *Biomacromolecules*, *5*(5), 1775–1786.
Vermeylen, R., Goderis, B., Reynaers, H., & Delcour, J. A. (2005). Gelatinisation related structural aspects of small and large wheat starch granules. *Carbohydrate Polymers*, *62*(2), 170–181.
Waigh, T. A., Gidley, M. J., Komanshek, B. U., & Donald, A. M. (2000). The phase transformations in starch during gelatinisation: A liquid crystalline approach. *Carbohydrate Research*, *328*(2), 165–176.
Wang, L., Xie, B., Xiong, G., Du, X., Qiao, Y., & Liao, L. (2012). Study on the granular characteristics of starches separated from Chinese rice cultivars. *Carbohydrate Polymers*, *87*, 1038–1044.
Zhao, K. S. (2008). *The dielectric spectroscopy method and application*. Beijing: Chemical Industry Press.
Zhao, H., Dong, B. Z., Guo, M. F., Wang, L. S., Qiao, J., Li, Z. H., et al. (2002). Determination of average thickness of transition layer of crystal polymer by small angle X-ray scattering. *Nuclear Techiques*, *25*, 837–840.
Zhu, Y. P. (2008). *Small-angle X-ray scattering: Theory, test, calculation, application*. Beijing: Chemical Industry Press.